Autoionizing emission from $3p^5 3d^{n+1} 4s^2$ states of Ca, Sc, Ti and V, excited by ion impact on solid targets

1999 J. Phys.: Condens. Matter 11 5723

(http://iopscience.iop.org/0953-8984/11/30/305)

J. Phys.: Condens. Matter **11** (1999) 5723–5734. Printed in the UK PII: S0953-8984(99)01194-7

Autoionizing emission from $3p^5 3d^{n+1} 4s^2$ states of Ca, Sc, Ti and V, excited by ion impact on solid targets

K F Kam, T E Gallon, J A D Matthew and C Kersten

Department of Physics, University of York, Heslington, York YO10 5DD, UK

Received 22 January 1999, in final form 12 May 1999

Abstract. Electron emission spectra of metallic Ca, Sc, Ti and V excited by rare-gas-ion bombardment are presented. The spectra display distinctive atomic characteristics as well as solid-state structure due to $M_{23}VV$ Auger emissions. By energy considerations, we show that their main spectral features can be explained by atomic autoionizations of the excited metal atoms in $3p^5 3d^{n+1} 4s^2$ states with excitation energies less than the solid-state 3p ionization energy. The relative importance of the autoionization channels $M_{23}N_1N_1$, $M_{23}M_{45}N_1$ and $M_{23}M_{45}M_{45}$ is investigated by comparing theoretically calculated spectra with the experimental spectra. Our work suggests that $M_{23}M_{45}N_1$ transitions rather than super-Coster–Kronig $M_{23}M_{45}M_{45}$ transitions dominate the decay channels.

1. Introduction

Electron emission and core-electron excitation by energetic noble-gas-ion bombardment on solids has long been studied because of its prototypical role in understanding the collision excitation mechanism, and for potential applications in surface science analysis (Valeri 1993). Ion-induced electron emission spectra can often reveal new and distinct features as compared to electron- and photon-excited spectra. The new information gained from ion-impact excitation is not only due to the different collisional cross sections between the probing source and the target, but because their excitation mechanisms can be fundamentally different. One of the most distinctive effects of ion-impact excitations is the potential for large momentum transfer between the energetic ion beams and the target particles, leading to the ejection of excited particles from the surface of the solid target. Subsequent decay of these sputtered particles often leads to 'atomic-like' electron emission spectra, although most studies have not resolved multiplet structure. In this paper we examine ion excitation of clean metallic Ca, Sc, Ti and V, to report the decay of atomic $3p^5 3d^{n+1} 4s^2$ states not normally observed in photon spectroscopy and to gain insight into how d screening of core holes contributes to the neutralization of ions created from ion bombardment.

The electron emission spectrum from Ca metal excited by rare-gas-ion bombardment has been explained by the decay of neutral excited atoms from $3p^5 3d4s^2$ states (Matthew *et al* 1997). This excited configuration is believed to have been formed from initial 3p bombardment-induced ionization followed by neutralization as a result of d-electron screening by conduction electrons in the solid (Cole *et al* 1995) and subsequent emergence from the surface in an excited atomic state. Hence, the energetics is such that only energy levels of the $3p^5 3d4s^2$ multiplet which have excitation energies less than the 3p-metal ionization energy of the Ca metal (i.e. ^3P and ^3F) can provide the initial state for emission. If an excited atom leaves the

0953-8984/99/305723+12$30.00

surface, electrons emitted via autoionization decay could then be detected, but at energies well below those observed in resonant photoemission where dipole selection rules control which terms in the multiplet are accessed. Previous work on ion-excited emission from Ti (Gallon *et al* 1995) suggest that a similar mechanism may be applicable to Ti.

In this paper, new ion-excited electron spectra of Sc and V metals are presented. The ion-excited electron spectra of Sc and Ti are notable for the absence of the higher-energy peaks observed in the photon- and electron-excited spectra (Meyer *et al* 1986); the hypothesis tested here is that ion-excited Ca, Sc, Ti and V autoionize from $3p^5 3d^{n+1} 4s^2$ states (with $n = 0, 1, 2, 3$ for Ca, Sc, Ti and V respectively) which lie *below* the 3p-metal ionization energies (I_{3p}) of the respective metals. Thus, transitions from the upper energy terms of the multiplet are prevented. For Ca, two autoionization channels $M_{23}M_{45}N_1$ and $M_{23}N_1N_1$ leading to a singly ionized $3p^6 4s^1$ and $3p^6 3d^1$ Ca^+ final states can occur (figure 1). For Sc, Ti and V, there is an additional autoionization channel $M_{23}M_{45}M_{45}$ leading to the final singly ionized state of $3p^6 3d^{n-1} 4s^2$ (hereafter, the subscripts denoting these decays will be dropped for convenience). The role of the MMM, MMN and MNN channels is systematically investigated and we show that our theory for electron emission from ion-impact excitations can account for the strongest features of the ion-excited spectra of Ca, Sc, Ti and V.

2. Experimental procedure

Details of the experimental apparatus and calibration methods have been published previously (Gallon *et al* 1995, Matthew *et al* 1997). Targets were cut from high-purity metal foils, except for the case of Ca where the target was prepared by *in situ* evaporation. The surface cleanliness was monitored by electron-induced AES. Ar, Kr and Ne ions of energy range of between 3 to 5 keV were used to excite the target. The ion gun was operated with an ionizing electron energy of 100 eV so the incident ion beam contained a mixture of singly and multiply ionized species. The ions were incident at a glancing angle of 20° and electrons collected at an emergence angle of 15° to the surface. The experimental geometry is therefore strongly forward-scattering biased which emphasizes emission from core-excited atoms outside the surface region rather than deep inside the solid. The shapes of the spectral peaks were not strongly dependent on incident angle in the range 25° to 10°. The electron spectra did not depend on the incident ion species and they are presented after subtraction of a smooth background curve as described by Gallon *et al* (1995). The spectrometer used was a concentric hemispherical analyser operated in a constant-pass-energy mode. The instrumental full width at half-maximum (fwhm) was constant over the energy range 10–20 eV with a value of ∼0.4 eV. The emitted electron energies are referenced to the vacuum level, but calibration is likely to be accurate to no better than 0.5 eV. The electron spectra from the target are represented by the solid curves in figure 2 and also in figures 4 to 7 (see later for a discussion).

3. Model and calculations

3.1. The model and some background discussion

The creation of the excited neutral atomic state $3p^5 3d^{n+1} 4s^2$ by ion bombardment can be summarized quasi-atomically:

$$3p^6[3d^n 4s^2] \rightarrow 3p^5[3d^n 4s^2] \rightarrow 3p^5[3d^n d^* 4s^2] \rightarrow 3p^5 3d^{n+1} 4s^2 \qquad (1)$$

where the square brackets denote that the valence electrons are in the metallic state. The first arrow indicates 3p-bombardment-induced ionization from ion impact. The fact that the

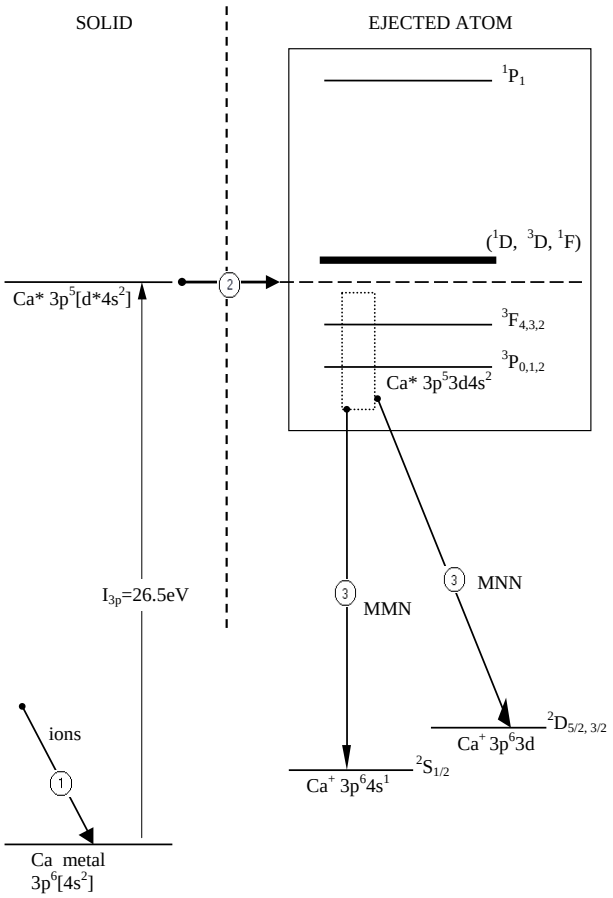

Figure 1. A schematic diagram of the processes leading to electron emission from ion-excited Ca metal: (1) 3p ionization induced by ion collision in or near the surface, followed by rapid neutralization by d screening electrons from the conduction band, (2) sputtered atoms emerging from the metal surface in a neutral excited state and (3) electron emissions via $M_{23}M_{45}N_1$ and $M_{23}N_1N_1$ autoionization for atoms which are on or have escaped from the surface.

electron spectra obtained are insensitive to the bombarding ion suggests that target–target (i.e. Ca–Ca, Sc–Sc, Ti–Ti or V–V) collisions are responsible for the ionization. From symmetry considerations and the electron-promotion model of Barat and Lichten (1972), the diabatic collision of the target atoms leads to electron promotion into a $5f\sigma$ state, which is different in symmetry from molecular states involving 3d electrons; thus collisions unambiguously lead to ionization rather than excitation. Ion-impact excitation of the metals is fundamentally different from resonant photon or electron excitations, because, in the latter, single-step direct quasi-atomic excitation to the excited $3p^53d^{n+1}4s^2$ state is competitive with direct ionization.

The second arrow indicates rapid neutralization by d screening from conduction band electrons, as in photoionization of alkaline-earth and transition metals (Cole *et al* 1995). Finally, the third arrow indicates the emergence of the neutral excited atoms from the metal surface due to sputtering, where only screened states of the $3p^53d^{n+1}4s^2$ multiplet with excitation energies less than the 3p-metal binding energy (I_{3p}) are accessible.

Thus, the available (initial) states are determined by the value of I_{3p} (Cardona and Ley 1978) which is measured relative to the Fermi level and the multiplet structure of the excited atom. The excited sputtered atoms could then theoretically autoionize via

$$3p^5 3d^{n+1} 4s^2 \longrightarrow \begin{cases} 3p^6 3d^{n-1} 4s^2 + e & \text{(MMM)} \\ 3p^6 3d^n 4s^1 + e & \text{(MMN)} \\ 3p^6 3d^{n+1} 4s^0 + e & \text{(MNN).} \end{cases} \tag{2}$$

The above processes, with the exception of the MMM transition, are clearly illustrated in figure 1 for the case of Ca metal.

Hence, our model implied that the most energetic autoionizing electron could potentially have a kinetic energy

$$E_{max} \simeq I_{3p} - I_{atom} \tag{3}$$

where I_{atom} is the first ionization energy of the atom (Sugar and Corliss 1978), giving $E_{max} = 20.4$, 21.8, 25.8 and 30.5 eV for Ca, Sc, Ti and V respectively. In practice, these energies would be altered slightly, because there is not always an initial atomic multiplet level which lies exactly equal to the 3p-metal ionization energy (see figure 1 for example). The value of E_{max} is indicated by an arrow on the energy axis of the spectra in figures 4 to 7 (later) where the top curve (solid curve) of each figure shows the experimental ion-induced electron emissions from Ca, Sc, Ti and V respectively. As expected, the values of E_{max} show general agreement with the maximum electron energy observed in the experimental spectra. A detailed discussion of the data in the figures is given later in the paper.

However, there is also present in the spectra of Sc to V a persistent and broad decaying structure on the high-energy side of the main peak which extends significantly beyond the maximum kinetic energy (E_{max}) of the autoionizing electrons. These structures are indicative of the presence of a small but significant bulk contribution. In particular, as observed from ion and electron excitations of transition metals (Xu *et al* 1993), $M_{23}VV$ Auger decay within the solid would be a likely source of the energetic electrons, where they will have a maximum kinetic energy determined by

$$E_{max}^{MVV} \simeq I_{3p} - \phi \tag{4}$$

where ϕ is the metal's work function ($\phi \approx 2.9$, 3.5, 4.5 and 4.3 eV for Ca, Sc, Ti and V respectively; Hagstrum 1981), giving $E_{max}^{MVV} = 23.6$, 24.8, 28.1 and 32.9 eV for Ca, Sc, Ti and V respectively. Both E_{max} and E_{max}^{MVV} are marked in figures 4 to 7 (see below). Note that, unlike the case for the electron-excited autoionizing emission, which is caused by a direct recombination following dipole-allowed 3p–3d transitions (Xu *et al* 1993, Bader *et al* 1983), where the higher-energy terms of the $3p^5 3d^{n+1} 4s^2$ multiplet are accessed, the high-energy contribution to our ion-excited spectra is exclusively due to the MVV Auger electrons rather than the autoionized electrons, as $E_{max}^{MVV} > E_{max}$. It is apparent that in the case of Sc, Ti and V, the maximum observed energy of the emitted electron seems to agree quite well with the values of E_{max}^{MVV}. For Ca, the highest observed energy of the electrons agrees well with E_{max} rather than E_{max}^{MVV}, implying that solid-state decays are not significant.

Xu *et al* (1993) studied the same metal targets with a much more powerful ion beam (14 keV Ar^+) in a less forward-scattering regime. The ion-excited electron spectra that they have obtained (figure 3 in the paper by Xu *et al*) are mainly due to $M_{23}VV$ band-like structure in an energy range which is just less than the energy associated with the autoionization emission observed in electron-impact excitations. Furthermore, they argue that the 'binding energy' of the extra 3d electron in the $3p^5 3d^{n+1} 4s^2$ configuration is generally less than the metal surface work function ϕ, so excited neutral states cannot be formed outside the surface. However, our

proposed model for electron emission allows autoionization from the lower energy levels of the excited $3p^5 3d^{n+1} 4s^2$ neutral atom whose excitation energy is less than I_{3p}. In the terminology of Xu *et al* this implies an 'effective 3d binding energy' greater than ϕ, but in contrast takes proper account of multiplet structure. In fact, the energy range of the MVV band structure in Xu's spectra overlaps with the energies of the peak structures in our spectra, suggesting a superposition of MVV transitions with some atomic autoionization features, which are less strong, because of their experimental geometry.

In addition to the above imposed energy 'limits', the structures of our ion-induced electron spectra are also distinctively different from photon- or high-energy-electron-excited spectra. In figure 2, we compare our ion-excited spectra (solid curves) for metallic Sc and Ti with the corresponding 'white-radiation' photo-excited spectra (dashed curves) for free atoms (Meyer *et al* 1986). This leads both to photoionization followed by Auger emission and excitation leading to autoionization. In the case of Ca (Bizau *et al* 1987), excitation is by non-resonant x-rays leading to Auger emissions only. The free-atomic spectra have been broadened by Gaussians with fwhm of 0.8 eV to take some account of the environment of the sputtered atoms. These spectra disagree with our results because ion-impact excitations give rise to different initial and final states of the atom by comparison to the states induced from photon or electron excitations. For electron energies of up to ∼19, 24 and 26 eV for Ca, Sc and Ti respectively, the photon-excited spectra shown are due to Auger decay of 3p holes in the singly ionized atom. Above 19 eV for Ca, the rather weak electron emission is due to photoemission of the Ca atoms' outer shells. However, strong autoionizing electron intensity is observed at around 25 eV in resonant photo-excitation of the $3p^5 3d^1 4s^2\ {}^1P$ state of Ca, which is again at a different energy to that in the ion-excited case. For Sc and Ti, the structures above these energies are due to autoionization emission from the upper terms of the $3p^5 3d^{n+1} 4s^2$ multiplet arising from direct dipole-allowed $3p \rightarrow 3d$ excitations which are wholly absent under ion bombardment.

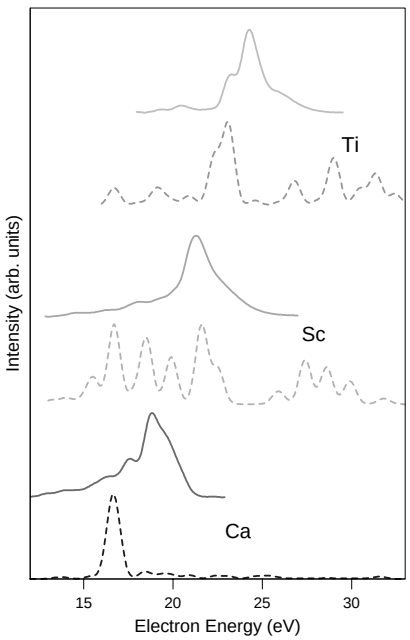

Figure 2. Comparisons of ion-induced electron spectra (solid curves) of metallic Ca, Sc and Ti with photon-excited electron spectra (dashed curves) of atomic Ca, Sc and Ti.

3.2. Calculations

Predictions of the electron emission energy are deduced from the difference in the energies of the initial and final states. Only a very small subset of experimental energies are available for the initial-state $3p^5 3d^{n+1} 4s^2$ terms of the excited atoms, e.g. in Sc (table 3 of Sonntag and Zimmermann 1992) and Ti (table 2 of Meyer *et al* 1986). They correspond to dipole-allowed transitions involving terms in the upper energy range of the multiplet which have the largest oscillator strengths. Thus, in order to obtain the energies of initial states corresponding to the lower terms in the multiplet, we use the atomic structure program MCDF (for multi-configuration Dirac–Fock) of Grant *et al* (1980) which enables the energy levels of most atomic configuration to be calculated. For Ca, the single-configurational values of the six lowest terms ($^3P_{0,1,2}$, and $^3F_{4,3,2}$) of the excited Ca* state ($3p^5 3d^1 4s^2$) are in good agreement with experiment (Bizau *et al* 1987). However, the single-configuration Dirac–Fock (DF) calculations would not produce sufficiently precise energies for the lower energy levels of the 3p-excited multiplet in all cases. To obtain a more accurate determination of these energies, we used a semi-empirical procedure, where the available experimental data are plotted against the energies calculated from a two-configuration calculation which gives oscillator strengths for dipole transitions between the states $3p^6 3d^n 4s^2$ and $3p^5 3d^{n+1} 4s^2$. The experimental transitions are identified with corresponding theoretical transitions with strong optical oscillator strength. An approximate linear relationship may be inferred between the experimental values and the theoretical values, as shown in figure 3, where we can by extrapolation obtain better estimates of the atomic transition energies in the lower-energy region. The arrow in figure 3 indicates that the lowest-energy $3p^5 3d^2 4s^2$ state of Sc* is 28 eV above the ground state of the unexcited Sc atom, approximately 1 eV higher in energy than the computed value. The corresponding correction for Ti is 1.2 eV.

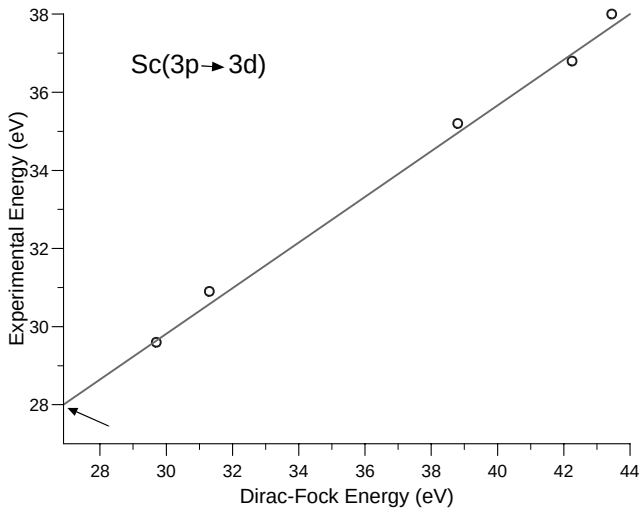

Figure 3. The semi-empirical estimate for excitation energies of Sc(3p → 3d) transitions. The arrow indicates that the lowest transition is at 28 eV, approximately 1 eV greater than the Dirac–Fock value.

Table 1 shows the values of I_{3p}, the number of accessible terms N_{3p} (which includes counting the J-states) in the excited atomic multiplet $3p^5 3d^{n+1} 4s^2$, the corresponding component terms under the LS-coupling scheme (J-values not shown) and the energy difference

Table 1. Important parameters in specifying accessible $3p^5 3d^{n+1} 4s^2$ terms. I_{3p} is the metal ionization energy; N_{3p} is the number of terms in the excited atomic multiplet $3p^5 3d^{n+1} 4s^2$ which participates in the de-excitation process. The next row gives the corresponding terms (or their amalgam) and ΔE_{3p} is the energy range of the accessible multiplet. $\delta N'_{3p}$ and $\Delta E'_{3p}$ are respectively the extra number of terms which may become accessible and the new energy range of the accessible multiplet if the effective value of I_{3p} is increased by 0.5 eV.

	$_{20}$Ca	$_{21}$Sc	$_{22}$Ti	$_{23}$V
I_{3p} (eV)	26.5	28.3	32.6	37.2
N_{3p}	6	4	11	15
Accessible terms	(^{3}P, ^{3}F)	^{4}D	(^{5}F, ^{5}D)	(^{6}D, ^{6}F, ^{4}D)
ΔE_{3p} (eV)	1.0	< 0.1	0.9	2.2
$\delta N'_{3p}$	0	0	5	5
$\Delta E'_{3p}$ (eV)	1.0	< 0.1	1.7	2.7

(ΔE_{3p}) between the lowest-energy term and the N_{3p}th term. Also shown is the extra number of terms ($\delta N'_{3p}$) which lie within 0.5 eV above I_{3p}, and the energy difference ($\Delta E'_{3p}$) between the lowest-energy term and the ($N_{3p} + \delta N'_{3p}$)th term. The quantities N'_{3p} and $\Delta E'_{3p}$ give some insight into the sensitivity of the electron emission energy to the values of I_{3p} which control the initial autoionizing states. For example, the combined effects of experimental uncertainties, spin–orbit splitting, core-level broadening and surface-state effects may increase the effective value of I_{3p} by up to 0.5 eV. For both Ti and V, an extra five terms from the excited Ti* and V* multiplet would be involved and there would be a subsequent increase in the range of electron emission energy by 0.8 eV for Ti and 0.5 eV for V.

For the final ionic states of Ca^+, Sc^+ Ti^+ and V^+, empirical data (Moore 1971, Sugar and Corliss 1978, 1979a, b) are available for almost all of the energy levels. Only three terms corresponding to the $^1S_0$ states of V^+ ($3p^6 3d^4$, $3p^6 3d^2 4s^2$) and Sc^+ ($3p^6 3d^2$) are not available, but their values were easily deduced from the semi-empirical procedure described earlier. The electron emission energies are calculated from the difference in the energies of the initial and final states. Ideally a full term-based transition matrix element analysis should be carried out, but this is very difficult for such open-shell systems. Hence, in our calculation, we have assumed that all of the terms of the multiplet structure in both the initial and final states are given equal weighting i.e. all the J-states are included equally. Other weighting schemes ($2J + 1$ weighting, initial-state weighting only etc) have be envisaged, and do not significantly change the present results when the individual transitions are broadened. Each transition is then convoluted by a Gaussian of fwhm $= 1.2$ eV to simulate broadening from instrumental and physical effects such as Doppler broadening of emitting atoms, inelastic scattering due to electron–hole pair creation at the surface and atoms emitting at different heights above the surface involving variation in interaction with induced image charges in the metal. Note that Lorentzian or lifetime broadenings have not been explicitly included in our simulation because the M_{23} core-hole lifetime only contributes a Lorentzian fwhm of $\lesssim 0.2$ eV (Fuggle and Alvarado 1980). The Gaussians are then superposed to give a spectrum for each of the individual autoionization processes.

The relative importance of the MMM, MMN and MNN spectra obtained should be related to their corresponding transition probabilities. These can be deduced from the M-shell Auger transition rates of Yin *et al* (1974, 1978) who calculated them from Hartree–Slater wavefunctions with X_α exchange, in neutral-atom potentials with calculated free-atom Auger energies. Their calculated rates agree remarkably well with experimental results obtained for

solids in the elemental range $25 \leqslant Z \leqslant 40$ (Yin *et al* 1974, 1978, Fuggle and Alvarado 1980, Schmidt *et al* 1984) confirming that super-Coster–Kronig MMM intensities were severely overestimated in previous predictions (McGuire 1972a, b).

Theoretical autoionizing M_{23} transition rates for excited atoms with the configuration $3p^5 3d^{n+1} 4s^2$ are shown in table 2 assuming that autoionization rates for elements of atomic number Z are approximated by the Auger transition rates of the $Z + 1$ atom with an extra nuclear charge and d electron. This assumption can be supported from the transition rates of Yin *et al* which show that for $Z \lesssim 32$, the MMM transition rate increases much faster than that for MMN transitions, in rough accordance with the statistics of the number of 3d electrons involved in the transition; i.e. the transition rates are directly related to the number of 3d electrons (n_{3d}) such that $\Gamma(\mathrm{MMN}) \propto n_{3d}$ and $\Gamma(\mathrm{MMM}) \propto n_{3d}(n_{3d} - 1)$. The experiments of Schmidt *et al* (1984) on the fast-electron excitations of atomic Cr, Mn, Fe and Co also confirm increasing dominance of the MMM autoionizations in the electron emission. The rates for V^* were deduced by interpolating the Auger data for V and Mn. No MNN transition rates are quoted in the paper by Yin *et al*, possibly confirming the generally held view that this transition is negligible compared to the other calculated transitions. The MNN transition, however, is a significant process in the autoionization decay of excited neutral Ca atoms (Bizau *et al* 1987) and in Auger emission from Sc (figure 2).

Table 2. Theoretical autoionizing $M_{2,3}$ transition rates ($\times 10^{-3}$ au) deduced from tables IX and X of Yin *et al* (1974, 1978).

	$_{21}Sc^*$ $(3p^5 3d^2 4s^2)$	$_{22}Ti^*$ $(3p^5 3d^3 4s^2)$	$_{23}V^*$ $(3p^5 3d^4 4s^2)$
$\Gamma(M_{23}M_{45}N_1)$	5.9	7.8	~ 9.4
$\Gamma(M_{23}M_{45}M_{45})$	1.6	5.5	~ 12.0

4. Results and discussion

In comparing free-atom theory with experiment it ought to be remembered that autoionization emission may be occurring close to the surface. Hence, the final ionized states are subjected to an image interaction which will produce both broadening and an average positive energy shift of $1/4z$ au ($\sim$0.7 eV) at a distance $z = 5$ Å from the metal surface.

4.1. Ca

In figure 4, the top curve (solid curve) is the experimental electron spectrum of Ca metal excited by 5 keV Ne ions. The spectrum contains a number of sharp atomic features at 20.1 eV, 19.1 eV, and 17.7 eV in good agreement with the electron energy of the autoionization mechanisms described above (see table 2 of Matthew *et al* 1997). Clearly, the higher terms have not participated in the autoionization process, or emission at significantly higher energy than 22 eV would be observed (see figure 1). The decay channels are then

$$3p^5 3d^1 4s^2 ({}^3P_{0,1,2}; {}^3F_{4,3,2}) \longrightarrow \begin{cases} 3p^6 3d^1 ({}^2D_{5/2,3/2}) + e & (\mathrm{MNN}) \\ 3p^6 4s^1 ({}^2S_{1/2}) + e & (\mathrm{MMN}). \end{cases} \quad (5)$$

There are no published data on the transition rates Γ(MMN) and Γ(MNN), but it is expected that $\Gamma(\mathrm{MMN}) > \Gamma(\mathrm{MNN})$ as there is more overlap between the 3p and 3d orbitals in the transition matrix elements than between the 3p and 4s orbitals. A transition rate ratio of $\Gamma(\mathrm{MMN}):\Gamma(\mathrm{MNN}) = 1.8{:}1.0$ gives a reasonable fit to the experimental spectrum. The

bottom curves in figure 4 show the electron emission curves for these individual channels, where the ratio of the areas under the MMN and MNN curves are proportional to their transition rate ratio. The middle curve is the sum of the MMN and MNN contributions, with its peak normalized to the peak of the experiment. This spectrum agrees with the experimental results for the main electron emission energy range, and the lineshape comparison appears to confirm the relative importance of the MMN and MNN autoionization channels. Finer agreement with the experimental spectrum may be possible by including autoionizing decays from other nearly degenerate neutral excited Ca configurations such as $3p^5 3d^2 4s$ or even $3p^5 3d^3$ (Sonntag and Zimmermann 1992, Bizau *et al* 1987). Auger emission from directly ionized Ca^+ $3p^5 4s^2 \rightarrow 3p^6$ + e are the likely cause of the weaker intensity observed below 16 eV.

4.2. Sc

Figure 5 shows the electron spectra for Sc metal excited by 4 keV krypton ions. The bottom curves show the theoretically calculated emission assuming the transition rate ratio of table 2. For completeness, the MNN decay is also shown with transition rate $\Gamma(\mathrm{MNN}) = \Gamma(\mathrm{MMM})/2$. Compared to that of Ca, the Sc experimental spectrum is relatively simple with the main peak at $E \approx 21.3$ eV which is easily identified with the MMN autoionization channels of decay. The broad structure on the low-energy side of this peak can be partly accounted for by the MMM channels, as shown in the middle curve which shows the sum contribution of the MMN

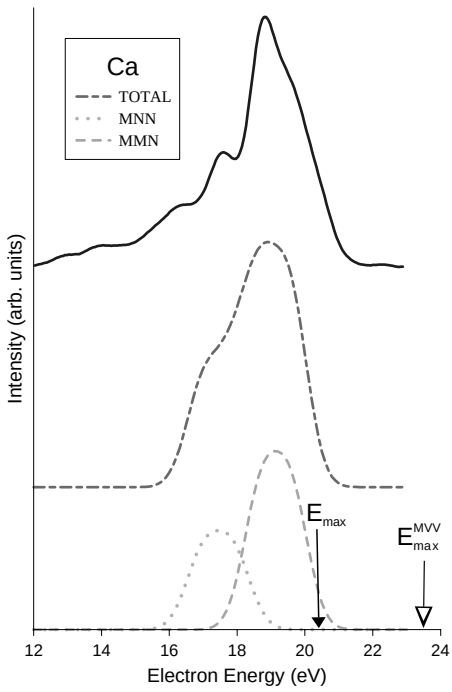

Figure 4. Comparisons of the experimental electron spectrum (solid curve) of ion-excited Ca metal with the calculated electron spectra (broken curves) due to autoionization from $3p^5 3d 4s^2$ states of Ca.

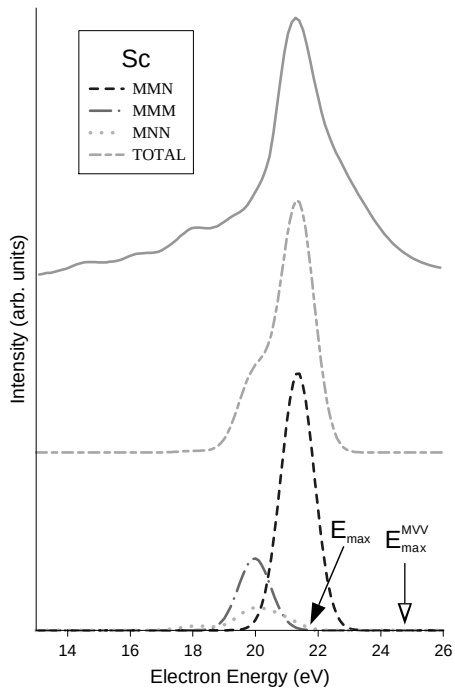

Figure 5. Comparisons of the experimental electron spectrum (solid curve) of ion-excited Sc metal with the calculated electron spectra (broken curves) due to autoionization from $3p^5 3d^2 4s^2$ states of Sc.

and MMM decays. This broad agreement with experiment indicates that the MMN decay is dominant over the MMM decay in roughly the ratio predicted by Yin *et al*. This contrasts with observations of fast-electron excitation of Sc and Ti metals (Meyer *et al* 1986), where the most prominent autoionization lines from dipole excitation seen for these metals are due to MMM decays. The weak structure below 19 eV in the experimental spectrum is probably due to Auger emissions of singly ionized Sc^+ ($3p^5 3d 4s^2 \rightarrow 3p^6 4s$ and $3p^6 3d$), as assigned by Meyer *et al* (1986).

4.3. Ti

Figure 6 shows the experimental spectrum (solid curve) for Ti metal excited by 3 keV krypton ions (Gallon *et al* 1995). The broken curves show the spectra for the three transition channels calculated using the transition rate ratios of table 2. The MNN transition is also shown for completeness, with its transition rate arbitrarily set at $\Gamma(\mathrm{MNN}) = \Gamma(\mathrm{MMM})$. As for Ca and Sc, the MMN decay seems to be the dominant channel, while surprisingly MMM emission occurs at energies inconsistent with experiment. The rates calculated by Yin *et al* take no account of multiplet structure and the matrix elements connecting the lower terms of the excited multiplet $3p^5 3d^{n+1} 4s^2$ to the final state may be weaker than for the average state. Hence, we propose that the MMM contribution to the electron emission must be significantly smaller than the prediction of Yin *et al* .

Although the MMN spectrum of figure 6 gives the correct electron energy range, the detailed structural comparison with the experimental spectrum is rather poor. A simple explanation may be that the term energies differ somewhat from the calculated structure, and that some transitions between the initial and final multiplets are more likely than others. Also, as is in the case of Ca, configuration interaction in Ti^* could have given rise to some additional initial autoionizing states which might accounts for the details of the experimental spectrum. It is of interest to note that the observed electron spectra of Sc and Ti of Meyer *et al* (1986) indicate that Auger MNN decays of a singly ionized atom actually surpass the MMN Coster–Kronig decay! Hence, the MNN autoionization emissions may not be as negligible as one might at first expect from simple wavefunction-overlap estimation of the transition matrix element.

4.4. V

Figure 7 shows the experimental spectra (solid curve) for V metal excited by 5 keV krypton ions, and the calculated spectra (broken curves) for the three transition channels assuming equal transition rates. The figure shows that the MMM decay route will lead to electron emissions at energies much lower than in the experiment and, as for Ti, must be far less significant than the theory would suggest. The MMN channels appeared to show good resemblance to the experimental spectrum, except that the entire calculated spectrum is up to about 1 eV too low in energy. This discrepancy may be accounted by a combination of factors:

(a) The experimental spectrum has an uncertainty of up to 0.5 eV due to calibration errors.

(b) The effective value of I_{3p} may be up to 0.5 eV larger as mentioned earlier. This would then allow more excitation channels and extend the maximum calculated energy of the emitted electrons by up to 0.5 eV (see table 1). The corresponding spectrum (not shown) would retain the overall shape of the MNN spectrum shown in figure 7, except for a slight shift in the peak structure toward higher energy and with a significantly broader slope at the higher-energy side.

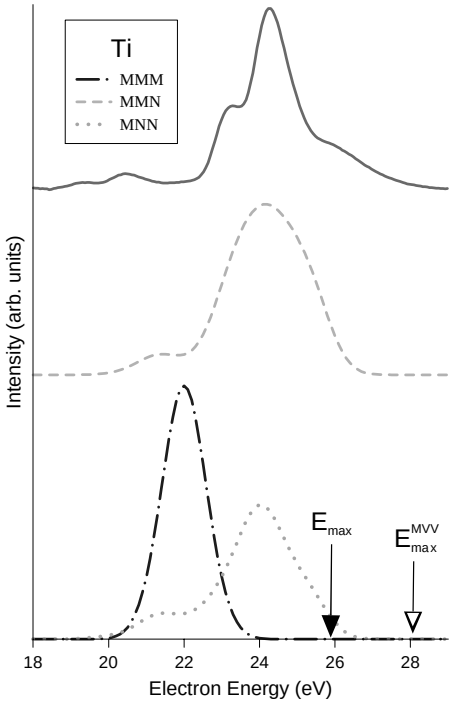

Figure 6. Comparisons of the experimental electron spectrum (solid curve) of ion-excited Ti metal with the calculated electron spectra due to autoionization from $3p^5 3d^3 4s^2$ states of Ti.

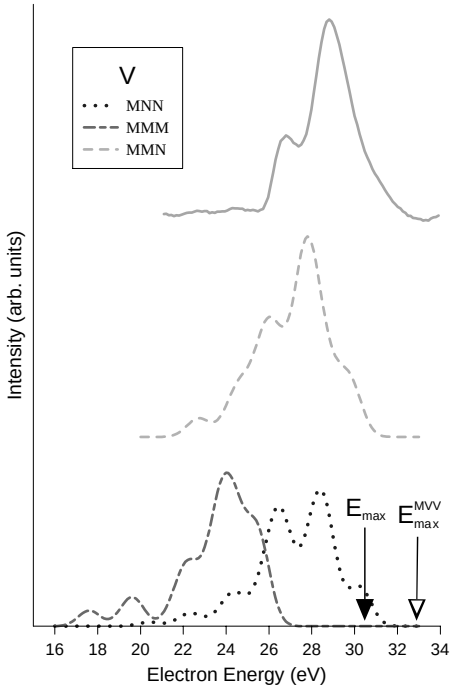

Figure 7. Comparisons of the experimental electron spectrum (solid curve) of ion-excited V metal with the calculated electron spectra due to autoionization from $3p^5 3d^4 4s^2$ states of V.

(c) Our calculations assume an upward correction of 1.4 eV to the lowest state of the excited V* configuration in the DF calculation plus a reduction of 30% in the energy of the higher levels. It is quite possible that these corrections should be increased slightly, thus shifting our calculated spectrum closer to the experimental results. A related effect is the enhanced electron correlation associated with the increase in the number of 3d electrons, coupled with the near degeneracy of the 3d and 4s levels. Hence, as in the 3p $\rightarrow$ 3d resonance of atomic Cr (Meyer *et al* 1986), the initial autoionizing state of the excited vanadium is likely to consist of configurations with an unfilled 4s shell, $V^*(3p^5 3d^5 4s)$ as well as $V^*(3p^5 3d^4 4s^2)$.

5. Conclusions

This paper has provided support for the view that ion-excited electron emission from metallic Ca, Sc, Ti and V in strongly forward-scattering geometry can lead to significant autoionization from energy levels of neutral $3p^5 3d^{n+1} 4s^2$ multiplets with excitation energies below that of the 3p ionization energy of the respective metals. The results imply a four-stage process:

(a) 3p ionization induced by ion impact,
(b) rapid neutralization by d screening near the surface,
(c) sputtering in the excited atomic states of the $3p^5 3d^{n+1} 4s^2$ configuration, restricted

energetically to the part of the multiplet structure which lies below the 3p ionization energy, and

(d) electron emission via autoionization processes leading to a singly ionized atom.

Comparisons of the calculated spectra with experiments show that MMN decay is the dominant channel for all of the metals studied here, contrary to established calculated transition rates and the emission pattern from high-energy electron- and photo-excited spectra of free atoms. The spectra also indicate that the MNN decay channel is an essential component in the autoionization process of Ca, though not necessarily significant for higher-Z metals.

The anomalies associated with the apparent lack of MMM transitions in Ti and V suggest that the transition matrix elements connecting the lower terms of the excited multiplet $3p^5 3d^{n+1} 4s^2$ to the final state may be particularly weak.

Acknowledgments

One of us (KFK) thanks the EPSRC for their financial support. Suggestions from the referees are also gratefully acknowledged.

References

Bader S D, Zajac G and Zak J 1983 *Phys. Rev. Lett.* **50** 1211
Barat M and Lichten W 1972 *Phys. Rev.* A **6** 211
Bizau J M, Gérard P, Wuilleumier F J and Wendin G 1987 *Phys. Rev.* A **36** 1220
Cardona M and Ley L 1978 *Photoemission in Solids I* (Berlin: Springer)
Cole R J, Brooks N J, Weightman P and Matthew J A D 1995 *Phys. Rev.* B **52** 2976
Fuggle J C and Alvarado S F 1980 *Phys. Rev.* A **22** 1615
Gallon T E, Orgassa J and Matthew J A D 1995 *J. Phys.: Condens. Matter* **7** 8539
Grant I P, McKenzie B J, Norrington P H, Mayers D F and Pyper N C 1980 *Comput. Phys. Commun.* **21** 207
Hagstrum H D 1981 *AIP 50th Anniversary Physics Vade Mecum* (New York: AIP) section 21
Matthew J A D, Gallon M A and Gallon T E 1997 *Phys. Rev.* B **55** 2697
McGuire E J 1972a *Phys. Rev.* A **5** 1043
McGuire E J 1972b *Phys. Rev.* A **5** 1052
Meyer M, Prescher Th, von Raven E, Richter M, Schmidt E, Sonntag B and Wetzel H E 1986 *Z. Phys.* D **2** 347
Moore C E 1971 *Atomic Energy Levels* NBS Circular No 467, vol 1 (Washington, DC: US Government Printing Office)
Schmidt E, Schröder H, Sonntag B, Voss H and Wetzel H E 1984 *J. Phys. B: At. Mol. Phys.* **17** 707
Sonntag B and Zimmermann P 1992 *Rep. Prog. Phys.* **55** 911
Sugar J and Corliss 1978 *J. Phys. Chem. Ref. Data* **7** 1191
Sugar J and Corliss 1979a *J. Phys. Chem. Ref. Data* **8** 1
Sugar J and Corliss 1979b *J. Phys. Chem. Ref. Data* **8** 865
Valeri S 1993 *Surf. Sci. Rep.* **17** 85
Xu F, Riccardi P, Oliva A and Bonanno A 1993 *Nucl. Instrum. Methods* B **78** 251
Yin L I, Adler I, Tsang T, Chen M H, Ringers D A and Crasemann B 1974 *Phys. Rev.* A **9** 1070
Yin L I, Adler I, Tsang T, Chen M H, Ringers D A and Crasemann B 1978 *Phys. Rev.* A **17** 1556 (erratum)